Catal Lett (2008) 126:20–30
DOI 10.1007/s10562-008-9627-x

Metal Phosphates as a New Class of Supports for Gold Nanocatalysts

Zhen Ma · Hongfeng Yin · Steven H. Overbury · Sheng Dai

Received: 5 August 2008 / Accepted: 22 August 2008 / Published online: 7 October 2008

Abstract Oxides and carbon are commonly used as supports for gold nanoparticles, but metal salts are barely considered as suitable supports. Our group recently communicated that gold nanoparticles supported on nanosized $LaPO_4$ (6–8 nm) are active for CO oxidation (Yan et al., Angew Chem Int Ed 45:3614, 2006). In the current work, we systematically developed an array of Au/M–P–O catalysts and tested them for catalytic activity and stability. It was found that 200 °C-pretreated Au/M–P–O (M = Ca, Fe, Co, Y, La, Pr, Nd, Sm, Eu, Ho, Er) show high CO conversions below 50 °C, and 500 °C-pretreated Au/M–P–O (M = Ca, Y, La, Pr, Nd, Sm, Eu, Ho, Er) show high CO conversions below 100 °C. These samples were characterized by ICP-OES, BET, XRD, TEM, SEM, and H_2-TPR. The stability of selected catalysts was studied as a function of time on stream. This work furnishes a new catalyst system for further fundamental and applied research.

Keywords Gold catalysis · CO oxidation · Activity · Metal phosphates · Nanoparticles

1 Introduction

Supported gold catalysts have many applications in ablating air pollutants, cleaning up H_2 streams, and synthesizing fine chemicals [1–5]. Most gold catalysts are prepared by loading gold on oxide supports via deposition-precipitation and other methods. In addition to the size of gold nanoparticles, supports also play a key role in determining activity. It has been suggested that gold on reducible supports (e.g., TiO_2, CeO_2, Fe_2O_3) exhibits higher activity in CO oxidation than gold on non-reducible supports (e.g., Al_2O_3, SiO_2) because the former can activate oxygen [6–8]. Nevertheless, properly prepared Au/Al_2O_3 [9–11] and Au/SiO_2 [12–19] can also show high activities in CO oxidation.

Although certain metal salts (e.g., sulfates, phosphates) are typical solid acid catalysts [20, 21], they have rarely been used to support gold nanoparticles. Lian et al. [22] found that $Au/BaCO_3$ is active for CO oxidation at room temperature, but it deactivates quickly on stream. Venugopal et al. and Phonthammachai et al. reported that $Au/Ca_{10}(PO_4)_6(OH)_2$ catalysts show activity in water-gas shift and CO oxidation above 100 and 50 °C, respectively [23, 24]. $Au/Ca_{10}(PO_4)_6(OH)_2$ catalyst is also useful for the wet oxidation of organic compounds in aqueous media [25]. Our group recently communicated that gold nanoparticles supported on nanosized $LaPO_4$ (6–8 nm) are active for CO oxidation below room temperature [26]. More recently, Li and coworkers [27] developed $Au/LaVO_4$ nanocomposite active for CO oxidation below 50 °C. However, the knowledge on the use of metal salts as supports for gold nanoparticles is still quite limited.

The previous work on Au/nano-$LaPO_4$ [26] prompted us to raise further questions. Considering that there are numerous metal phosphates, is it possible to use metal phosphates other than $LaPO_4$ to load gold nanoparticles? Are these metal phosphate-based catalysts active in CO oxidation, or is Au/nano-$LaPO_4$ [26] a unique case? Are these phosphate-based gold catalysts stable on stream? In

Electronic supplementary material The online version of this article (doi:10.1007/s10562-008-9627-x) contains supplementary material, which is available to authorized users.

Z. Ma · H. Yin · S. H. Overbury · S. Dai (✉)
Chemical Sciences Division, Oak Ridge National Laboratory, Oak Ridge, TN 37831, USA
e-mail: dais@ornl.gov

addition, considering that the homemade supports prepared using various methods under complicated conditions would lead to different particle sizes, crystal phases, morphologies, levels of residual ions from the synthesis mixture, and thus different catalytic performance, it is desirable to use commercially available supports for initial screening, while leaving the further optimization of catalysts the subject of further research.

Herein, a number of commercial metal phosphates were used as supports for loading gold via a deposition-precipitation method. The catalytic performance in CO oxidation was studied following catalyst pretreatment in O_2-He at 200 or 500 °C, and relevant characterization employing ICP-OES, BET, XRD, TEM, SEM, and H_2-TPR was carried out. Interestingly, gold nanoparticles can be well dispersed on many of these metal phosphate supports and show significant activities at room temperature. Since many metal phosphates are useful in acid catalysis and selective oxidation [20, 28–32], Au/metal phosphates developed here may be useful for many other reactions to be explored in the future. In addition, gold on chemically distinct supports may provide new opportunities for fundamental studies to elucidate the nature of active sites and reaction mechanisms.

2 Experimental

$HAuCl_4$, $Mg_3(PO_4)_2 \cdot xH_2O$, $AlPO_4$, $[Ca_5(OH)(PO_4)_3]_x$, $FePO_4 \cdot 2H_2O$, $Co_3(PO_4)_2$, $Zn_3(PO_4)_2$, YPO_4, $LaPO_4 \cdot xH_2O$, $PrPO_4$, $NdPO_4 \cdot xH_2O$, $SmPO_4 \cdot xH_2O$, $EuPO_4 \cdot xH_2O$, $HoPO_4$, and $ErPO_4 \cdot xH_2O$ were obtained from Aldrich. TiO_2 was Degussa P25. These materials were used as received, except that $NdPO_4 \cdot xH_2O$ and $SmPO_4 \cdot xH_2O$ were dried at 85 °C before testing their activities in control experiments or conducting H_2-TPR experiments. Zr–P–O support was prepared by dissolving 3.2 g $ZrOCl_2 \cdot 8H_2O$ in 100 mL deionized water followed by adding 100 mL 0.5 M H_3PO_4, magnetic stirring for 2 h, centrifuging, thorough washing by water, and drying.

Gold was loaded onto supports via a deposition-precipitation method [1–5]. One hundred milliliters of $HAuCl_4$ solution containing 0.6 g $HAuCl_4 \cdot 3H_2O$ was sampled into a beaker, and the pH value was adjusted to 10 by adding droplets of 1.0 M KOH with vigorous magnetic stirring and monitored with a pH meter. The resulting solution was heated at 80 °C, 2.0 g support added, the pH value readjusted to 10, and the slurry magnetically stirred for 2 h. Note that some metal phosphate supports may contain residual acids, so the pH value was readjusted to 10 during synthesis to remedy the decrease in pH value. After 2 h, the precipitate was centrifuged, washed four times with water, and dried at 40 °C for 2 days.

CO oxidation was tested in a plug-flow microreactor (Altamira AMI 200). Unless otherwise specified, 50 mg catalyst was loaded into a U-shaped quartz tube (4 mm i.d.) supported by quartz wool. The catalyst was pretreated online in flowing 8% O_2 (balance He) at 200 or 500 °C for 2.5 h. The catalyst was cooled down before the gas was switched to the reaction mixture (37 cm^3/min of 1% CO in air), and the reaction temperature was varied by immersing the U-shaped tube in cold-bath or a furnace. A portion of the product gas stream was extracted periodically with an automatic sampling valve, and analyzed using a dual-column gas chromatograph with a thermal conductivity detector.

Elemental analysis was conducted using inductively coupled plasma-optical emission spectroscopy (ICP-OES) on a Thermo IRIS Intrepid II spectrometer. BET surface areas were measured by N_2 adsorption-desorption at 77 K using a Micromeritics Gemini instrument. XRD data were collected on a Siemens D5005 diffractometer with Cu Kα radiation. TEM and SEM images were taken on a Hitachi HD-2000 STEM operating at 200 kV. H_2-TPR experiments were conducted using a Micromeritics AutoChem II chemisorption analyzer. The solid sample (50 mg) was flushed by 10% H_2 in Ar (50 mL/min) for 10 min, and then

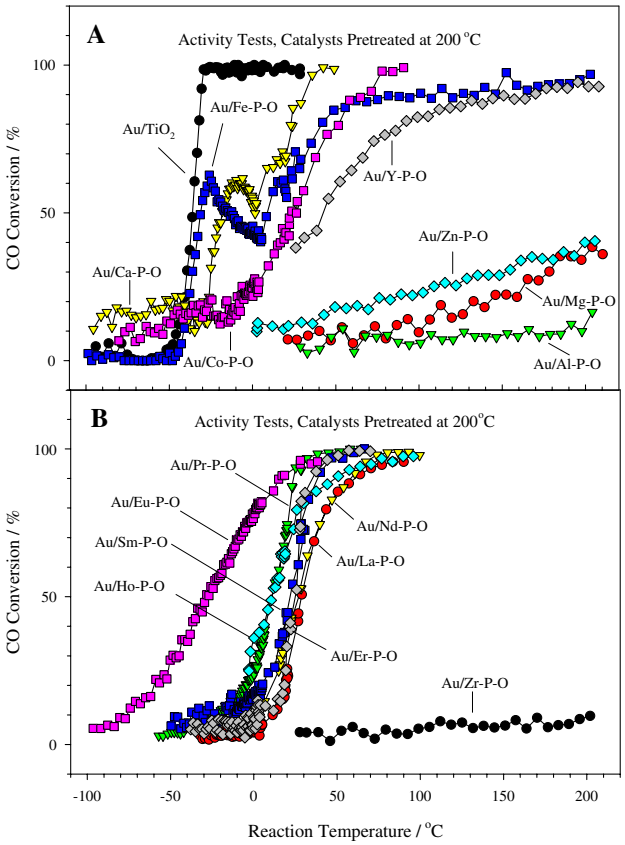

Fig. 1 CO conversion curves of 200 °C-pretreated Au/TiO_2 and Au/M–P–O catalysts

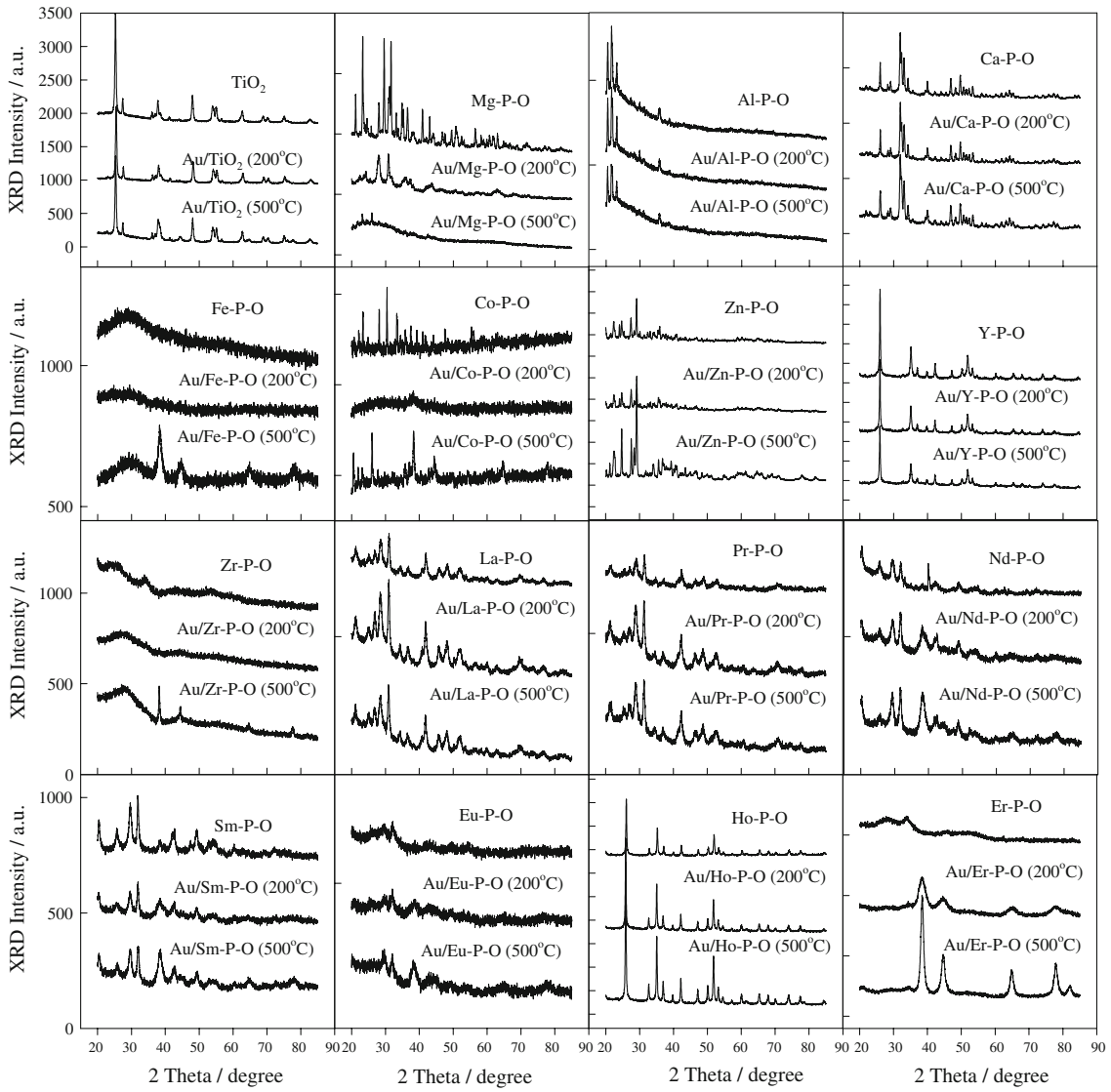

Fig. 2 XRD patterns of as-obtained TiO_2 and metal phosphates as well as Au/TiO_2 and Au/M–P–O catalysts collected after 200- or 500 °C-pretreatment and subsequent reaction testing

the temperature was ramped to 800 °C at a rate of 10 °C/min. The uptake of H_2 was recorded with the aid of a TCD detector.

3 Results and Discussion

3.1 Au/M–P–O Catalysts Pretreated in O_2-He at 200 °C

To run gas-phase catalytic reactions, it is necessary to pretreat catalysts at elevated temperatures to remove adsorbed water and volatile contaminants. Figure 1 summarizes CO conversion curves of catalysts that were pretreated at 200 °C. Au/M–P–O (M = Ca, Fe, Co, Y, La, Pr, Nd, Sm, Eu, Ho, Er) catalysts show high CO conversions when the reaction temperature is below 50 °C, whereas Au/M–P–O (M = Mg, Al, Zn, Zr) samples are poorly active below 200 °C. Therefore, certain metal phosphates other than $LaPO_4$ [26] can also be suitable supports for making active gold catalysts.

We first present the characterization of active catalysts (Au/M–P–O, M = Ca, Fe, Co, Y, La, Pr, Nd, Sm, Eu, Ho, Er). According to the XRD data in Fig. 2, the metallic gold peaks (2θ = 38, 44, 65, and 78°) of these 200 °C-pretreated catalysts are either quite broad (Au/M–P–O, M = Co, Nd, Sm, Eu, Er) or not appreciable (Au/M–P–O, M = Ca, Fe, Y, La, Pr, Ho), because the gold particles on these supports are either small or the gold contents are low [4]. According to our systematic electron microscopy

Table 1 Physiochemical properties and T_{50} values of Au/M–P–O and Au/TiO_2

	Surface area (m^2/g)	Gold loading (wt%)	T_{50} of 200 °C-pretreated sample (°C)	Gold size of 200 °C-pretreated sample (nm)	T_{50} of 500 °C-pretreated sample (°C)	Gold size of 500 °C-pretreated sample (nm)
1. Au/TiO_2	50	2.3	−36	2–8	140	5–30
2. Au/Mg–P–O	14	0.63	–	2–6	279	2–6, occasionally 12–40
3. Au/Al–P–O	79	0.31	–	2–4	–	3–10
4. Au/Ca–P–O	21	1.3	−18	2–5	16	2–5
5. Au/Fe–P–O	28	5.5	−31	1–3	244	2–20
6. Au/Co–P–O	2	5.0	24	2–3	362	4–18, occasionally 200
7. Au/Zn–P–O	3	2.4	–	2–5	–	4–12
8. Au/Y–P–O	54	2.4	42	2–6	22	2–5
9. Au/Zr–P–O	–	0.58	–	2–12, occasionally 30–50	–	10–65
10. Au/La–P–O	56	0.50	29	5–20	36	5–20
11. Au/Pr–P–O	57	0.90	11	3–8	−49	3–15
12. Au/Nd–P–O	77	11.8	27	2–5	82	3–12
13. Au/Sm–P–O	85	11.9	22	2–5	18	2–10
14. Au/Eu–P–O	61	8.5	–28	2–6	68	6–15
15. Au/Ho–P–O	24	0.66	11	2–7	62	2–15
16. Au/Er–P–O	206	20.4	25	3–6	58	5–12

experiments, the sizes of gold nanoparticles of these 200 °C-pretreated active catalysts are generally within a few nanometers (Table 1). For instance, gold nanoparticles (1–3, 2–6, and 3–6 nm, respectively) are well dispersed on Fe–P–O, Eu–P–O, and Er–P–O supports (Fig. 3). Therefore, some metal phosphates other than $LaPO_4$ can also be good supports for dispersing gold nanoparticles. Interesting is that some supports, such as Eu–P–O (Fig. 3d) and Er–P–O (Fig. 3f), have nanosized pore structures, contributing to the relatively high surface areas of Au/Eu–P–O (61 m^2/g) and Au/Er–P–O (206 m^2/g), whereas Fe–P–O support is relatively smooth (Fig. 3b), and the surface area of Au/Fe–P–O is relatively low (28 m^2/g).

After characterizing active catalysts, we then turn to inactive Au/M–P–O (M = Mg, Al, Zn, Zr) samples. The gold loadings of Au/M–P–O (M = Mg, Al, Zr) are low (0.63, 0.31, and 0.58 wt%, respectively, Table 1), possibly due to the low isoelectric points of these supports (e.g., the isoelectric point of Zr–P–O is about 4 [33]). However, their low activities may not be solely attributed to low gold loadings because: (1) For comparison, Au/M–P–O (M = La, Pr, Ho) catalysts have low gold loadings (0.50, 0.90, and 0.66, respectively), but they are much more active; (2) The gold loading of Au/Zn–P–O is relatively high (2.4 wt%), but it is still not particularly active; (3) We obtained high-gold-loading Au/Mg–P–O (8.6 wt% Au) and Au/Al–P–O (2.4 wt% Au) by adjusting the pH value of the $Au(OH)_xCl_{4-x}^-$ solution to lower values instead of 10. We additionally prepared Au/Al–P–O (3.9 wt% Au) by using $Au(en)_2Cl_3$ as the precursor according to the procedure used for the synthesis of Au/SiO_2 [18, 19]. These three samples are not particularly active, either (Fig. S1 in the Supporting Information).

As shown in Fig. 4a and b, gold nanoparticles with sizes of 2–4 nm and mostly 3 nm are well dispersed on the Al–P–O support. The gold particle sizes of 200 °C-pretreated Au/Mg–P–O (data not shown) and Au/Zn–P–O (e.g., Fig. 4c and d) are 2–6 and 2–5 nm, respectively. On the other hand, gold particles on 200 °C-pretreated Au/Zr–P–O have diameters of 2–12 nm, and 30–50 nm particles are occasionally seen (e.g., Fig. 4e and f). Therefore, although the big gold particle sizes of Au/Zr–P–O may play a role in the low activity of Au/Zr–P–O, the low activities of Au/M–P–O (M = Mg, Al, Zn) catalysts are clearly not due to the lack of small gold particles. In fact, Yan et al. [34] previously found that gold nanoparticles on zeolite $AlPO_4$-H1 are also not particularly active. Apparently, different phosphate supports are different for gold catalysis, which may be vaguely called "support effects". This could be due to different reaction mechanisms, different adsorption/activation modes of CO and O_2 on gold catalysts made of different supports, and other factors beyond the current understanding. Further infrared spectroscopic research is in progress to shed light on the reaction mechanisms and support effects [35].

3.2 Au/M–P–O Catalysts Pretreated in O_2-He at 500 °C

Although Au/M–P–O (M = Ca, Fe, Co, Y, La, Pr, Nd, Sm, Eu, Ho, Er) catalysts pretreated at 200 °C already show high CO conversions, we are curious about whether these

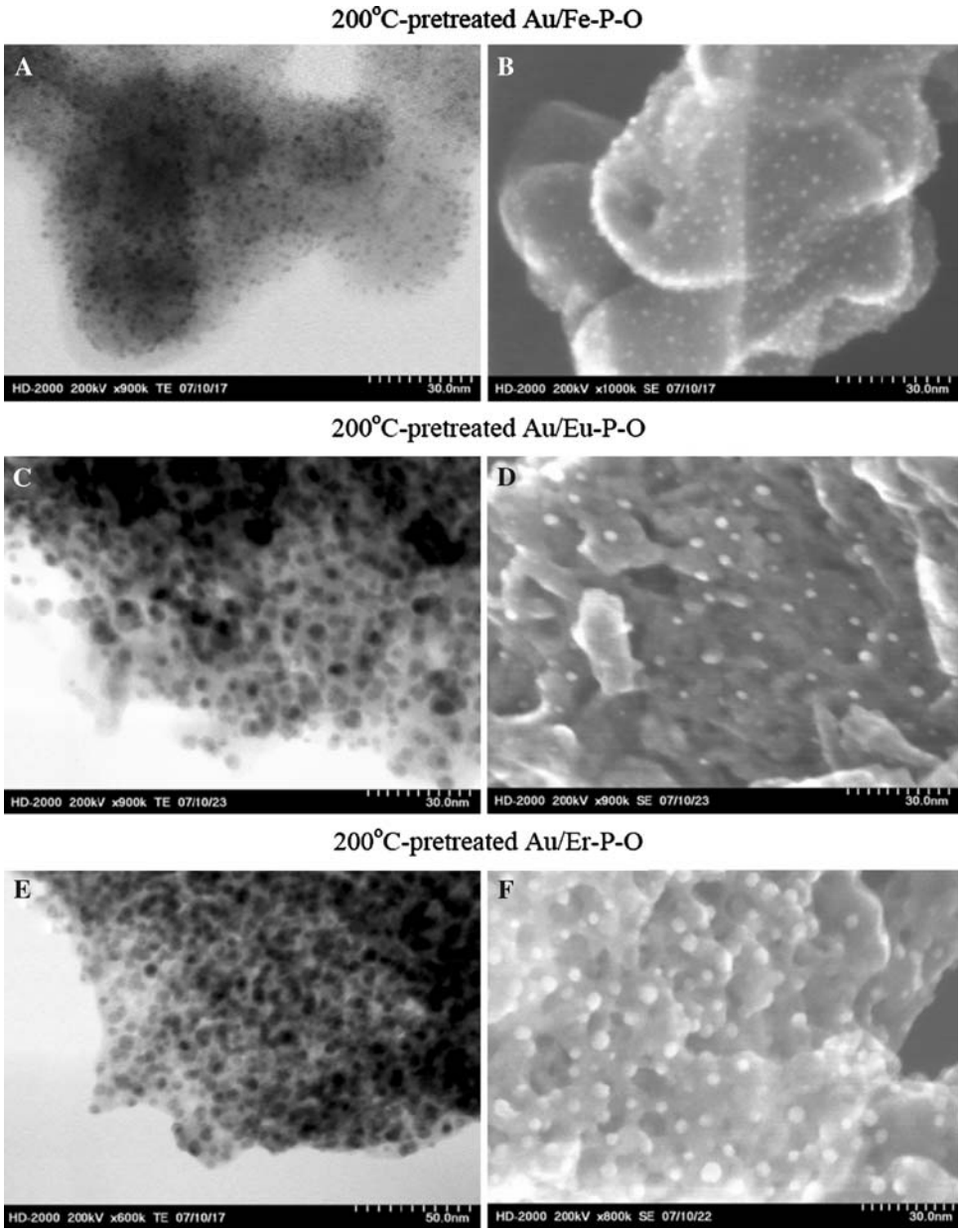

Fig. 3 Bright-field TEM (left) and SEM (right) images of Au/Fe–P–O (**a**, **b**), Au/Eu–P–O (**c**, **d**), and Au/Er–P–O (**e**, **f**) collected after 200 °C-pretreatment and subsequent reaction testing

catalysts are still active if they are pretreated at higher temperatures. This question is related to the thermal stability of gold catalysts in practical applications where high-temperature environments are encountered [36, 37]. The thermal behavior of supported gold nanoparticles is of fundamental interest as well [38, 39].

Figure 5 shows the CO conversions of gold catalysts pretreated in O_2-He at 500 °C. Au/M–P–O (M = Ca, Y, La, Pr, Nd, Sm, Eu, Ho, Er) catalysts still show high conversions below 100 °C, and Au/M–P–O (M = Mg, Al, Zn, Zr) are again not active below 200 °C. Compared with the corresponding 200 °C-pretreated samples, 500 °C-pretreated Au/M–P–O (M = Fe, Co) are much less active. Additional control experiments indicate that all of the neat metal phosphate supports are not active below 300 °C (Fig. S2). In contrast, although Au/TiO_2 shows high activity after 200 °C-pretreatment ($T_{50} = -36$ °C, Fig. 1a), its activity dramatically decreases ($T_{50} = 140$ °C, Fig. 5a) due to the sintering of gold nanoparticles [40–43].

We first address the relatively active catalysts (Au/M–P–O, M = Ca, Y, La, Pr, Nd, Sm, Eu, Ho, Er). According to the XRD data in Fig. 2, the gold peaks ($2\theta = 38$, 44, 65, and 78°) of 500 °C-pretreated Au/M–P–O (M = Ca, Y, La, Ho) catalysts are not appreciable, but the gold peaks of 500 °C-pretreated Au/M–P–O (M = Pr, Nd, Sm, Eu, Er) catalysts are clearly seen. According to the TEM data in Table 1, the gold particles sizes of the latter group are generally larger than those of the former. Typical TEM images of 500 °C-pretreated Au/M–P–O (M = Ca, Y) and Au/M–P–O (M = Nd, Sm) are presented in Figs. 6 and 7, respectively.

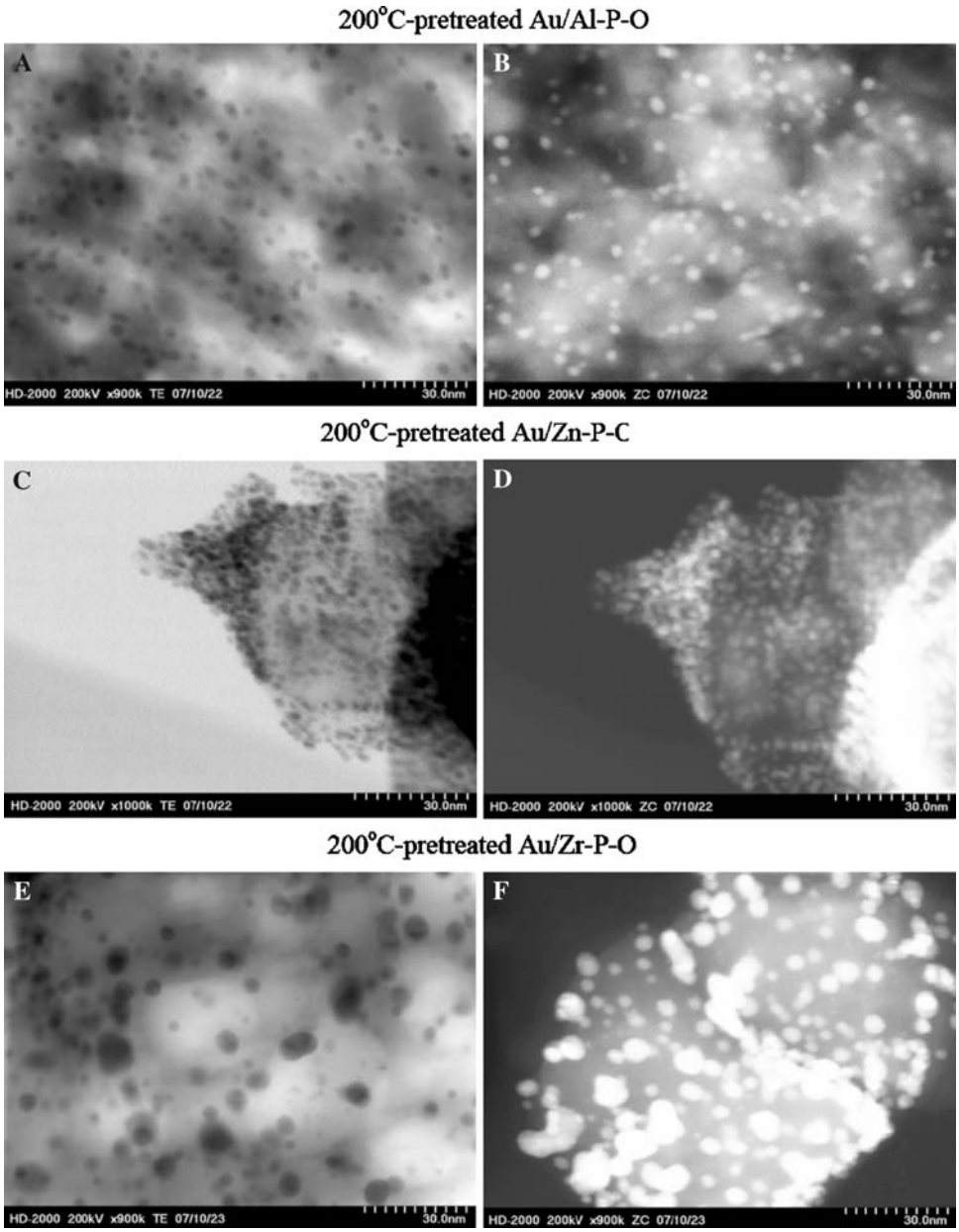

Fig. 4 Bright-field (left) and dark-field (right) TEM images of Au/Al–P–O (**a**, **b**), Au/Zn–P–O (**c**, **d**), and Au/Zr–P–O (**e**, **f**) collected after 200 °C-pretreatment and subsequent reaction testing

The gold nanoparticles on Ca–P–O and Y–P–O are small, in the range of 2–5 nm, whereas those on Nd–P–O and Sm–P–O are relatively bigger, in the range of 3–12 nm and 2–10 nm, respectively. Nevertheless, compared with that of Au/TiO_2, the sintering of active Au/M–P–O catalysts is less severe. The gold nanoparticles on TiO_2 are big (5–30 nm) after 500 °C-pretreatment (Table 1).

Next, we address the less active or relatively inactive catalysts (Au/M–P–O, M = Al, Fe, Co, Zn, Zr). As shown in Fig. S3, small gold nanoparticles are uniformly dispersed on Al–P–O and Zn–P–O support, whereas big gold particles are populated on Zr–P–O support. These TEM data are consistent with the XRD data (Fig. 2). It is noteworthy that 200 °C-pretreated Au/Fe–P–O and Au/Co–P–O are active (Fig. 1), whereas the 500 °C-pretreated samples are not particularly active (Fig. 5). XRD data show that the gold peaks of 200 °C-pretreated Au/Fe–P–O and Au/Co–P–O are not particularly obvious, whereas those of 500 °C-pretreated samples are obvious (Fig. 2), indicating the sintering of gold nanoparticles. The TEM data in Fig. S4 corroborate the XRD results.

3.3 H_2-TPR Characterization of Supported Gold Catalysts and Supports

Above, we reported the activity tests and ICP-OES, BET, XRD, TEM, and SEM characterization of a series of

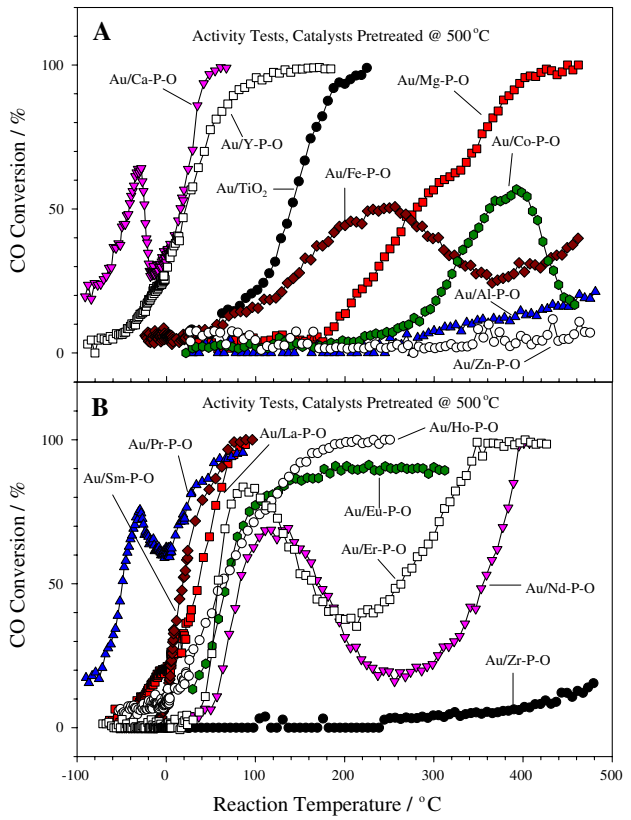

Fig. 5 CO conversion curves of 500 °C-pretreated Au/TiO_2 and Au/M–P–O catalysts

Au/M–P–O catalysts. Since we are using metal phosphates as a new class of supports for gold nanocatalysts, one relevant question refers to the reducibility of these metal phosphate supports. Therefore, H_2-TPR characterization of supports and as-synthesized gold catalysts was conducted. According to Fig. 8, there are obvious H_2 uptakes with standard CuO and Fe_2O_3 samples used for comparison, but the reduction of most of the bulk metal phosphates (except for Fe–P–O, Co–P–O, and Zn–P–O) is not obvious. This is consistent with the finding in the literature that Ca–P–O is not reducible [23] whereas Fe–P–O is reducible [44]. When gold is loaded onto metal phosphate supports, the reduction of gold cations below 200 °C is obvious when the gold contents of the samples (Au/M–P–O, M = Fe, Co, Zn, Nd, Sm, Eu, Er) are high (Fig. S5). The reducibility trend established using neat supports is still valid in the H_2-TPR experiments involving supported gold catalysts. Combining our catalysis results (Figs. 1 and 5) and H_2-TPR data (Figs. 8 and S5), it can be said that gold nanoparticles on non-reducible bulk metal phosphate supports can also be active for CO oxidation [23]. The question then arises: what is the role of reducible and non-reducible metal phosphate supports in catalytic CO oxidation? This is an interesting question desiring further research [35].

3.4 Stability Tests

The stability of gold catalysts as a function of time on stream should be sufficiently tested [45]. Figure 9 shows the room-temperature CO conversions on different 200 °C-pretreated gold catalysts as a function of reaction time. The CO conversions on most of these catalysts undergo deactivation or activation in the initial 20–30 h, and the conversions then stabilize afterwards during the testing periods. Such deactivation or reactivation is still observed when the catalysts are pretreated at 500 °C, and the catalysts are still relatively stable after reaching the steady state (Fig. S6). Most of the catalysts were sufficiently tested at room temperature for more than 70 h. We selected 200 °C-pretreated $Au/ErPO_4$ and tested the stability for a longer time. After 300 h on stream, the CO conversion is still 88%, compared to the 91% value at 30 h.

We explored the nature of the initial deactivation by doing further experiments. In one, Au/Ca–P–O was pretreated at 500 °C and cooled down to room temperature, and the stability was tested. The initial deactivation is very obvious. After the stability test, the catalyst was regenerated in O_2-He at 400 °C for 1 h and cooled down to room temperature for reaction. The initial deactivation is still observed and the steady-state conversion is the same as that in the first run (Fig. 10a). We carried out another experiment by testing the stability of 500 °C-pretreated $Au/PrPO_4$ (Fig. S6B), stored the used catalyst in the U-shaped quartz tube for 3 months, and then regenerated the catalyst in O_2-He at 400 °C and re-tested the stability. The initial conversion is 86%, compared to the 96% value of the catalyst in the first run, whereas the conversion at 72 h on stream is 65%, comparable to the 62% value of the catalyst in the first run. The fact that the deactivated catalysts may be partially regenerated following thermal treatment implies that such deactivation may be due to the slow build up of a certain type of carbonate or other surface species that can be eliminated at elevated temperatures [46–50]. Further infrared spectroscopic research is in progress to pin down the evolution of surface species during the course of reaction [35].

Finally, we obtained some preliminary information on the nature of the initial activation. In one, Au/Sm–P–O was pretreated at 500 °C and cooled down to room temperature, and the stability was tested. The initial increase in CO conversion is obviously seen. After the stability test, the catalyst was treated in O_2-He at 400 °C for 1 h and cooled down to room temperature for reaction. The initial activation process is again seen, and the steady-state conversion is consistent with the one in the first run (Fig. 10b). Although we cannot exclude other reasons such as the gradual reduction of cationic gold to metallic gold as seen in the case of Au/SiO_2 [51], we speculate that the

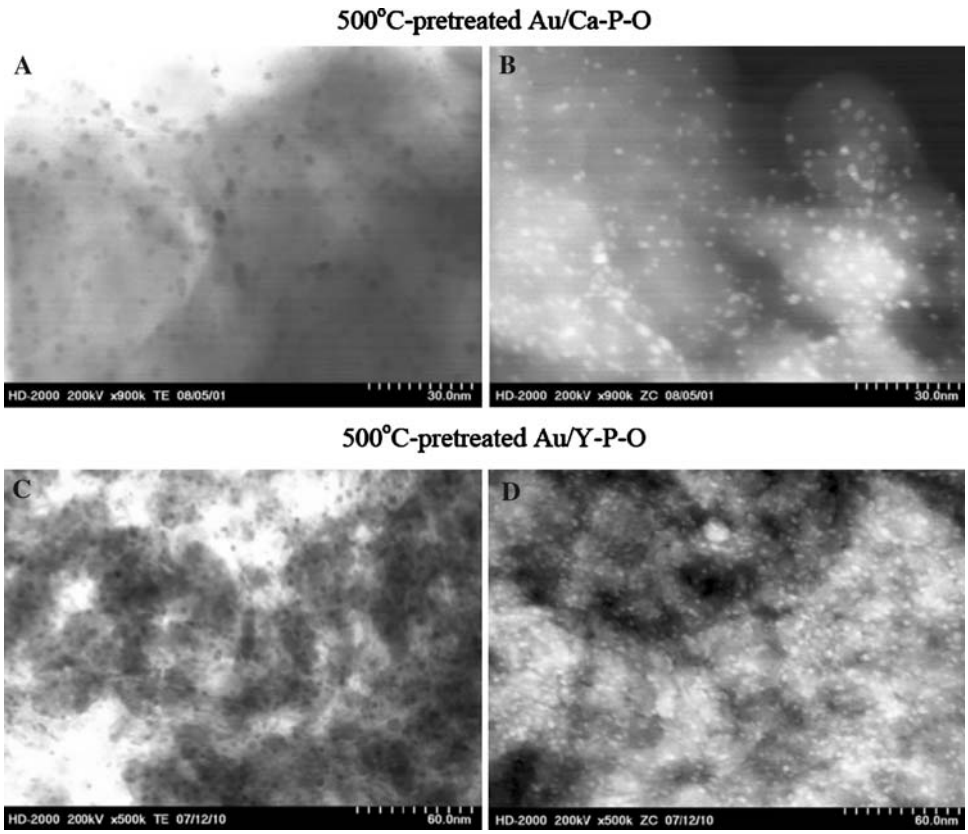

Fig. 6 Bright-field (left) and dark-field (right) TEM images of Au/Ca–P–O (**a**, **b**) and Au/Y–P–O (**c**, **d**) collected after 500 °C-pretreatment and subsequent reaction testing

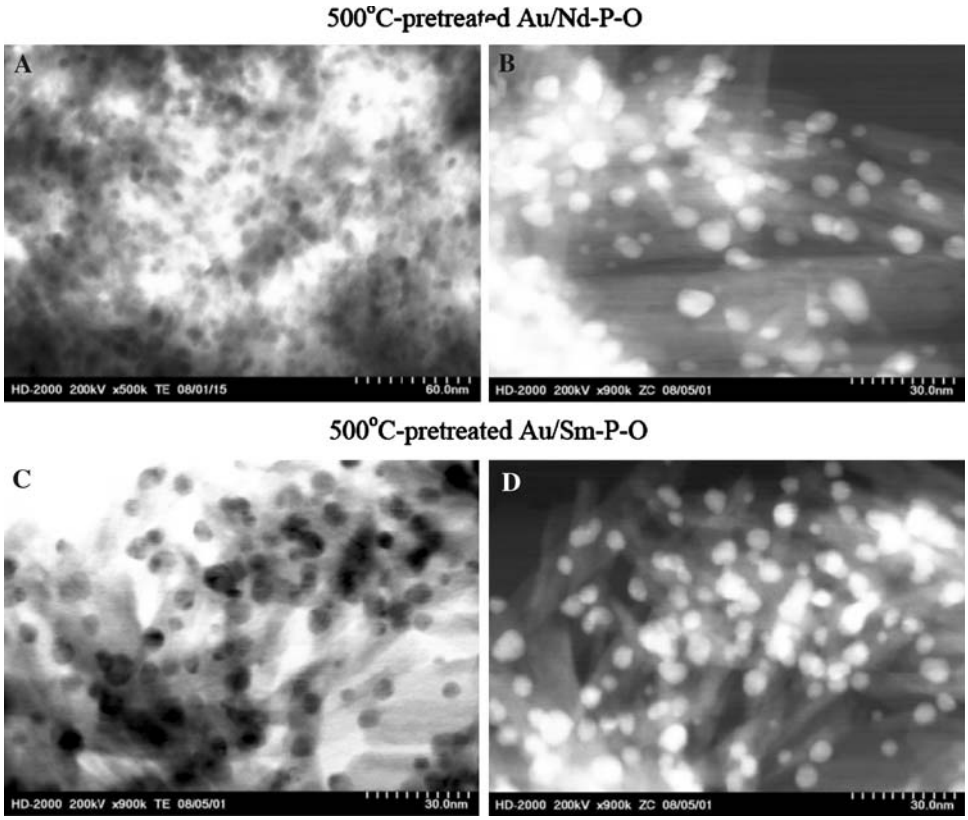

Fig. 7 Bright-field (left) and dark-field (right) TEM images of Au/Nd–P–O (**a**, **b**) and Au/Sm–P–O (**c**, **d**) collected after 500 °C-pretreatment and subsequent reaction testing

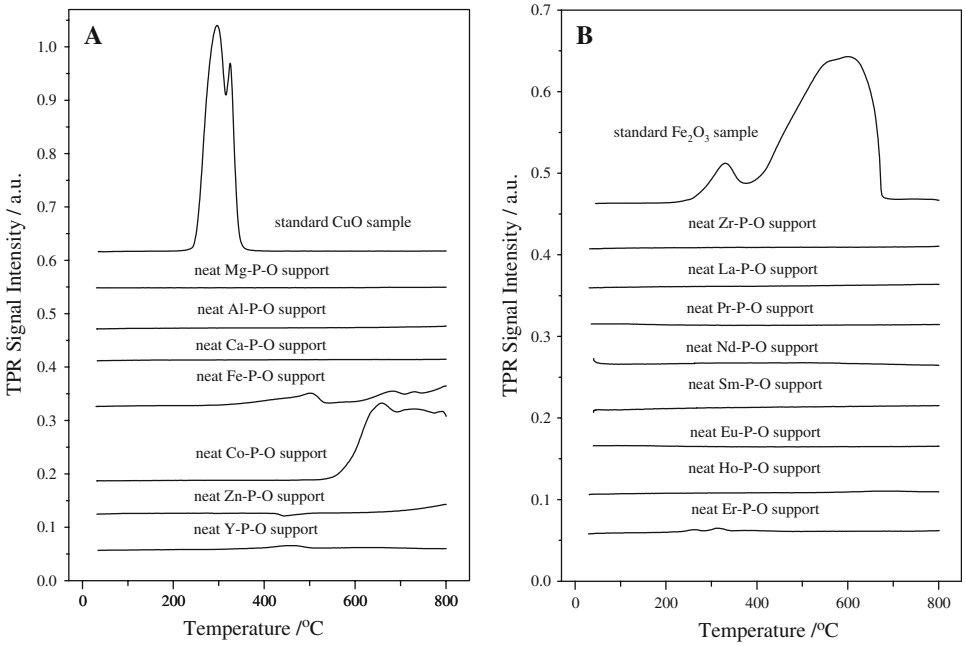

Fig. 8 H_2-TPR data of neat M–P–O supports and standard CuO and Fe_2O_3 samples

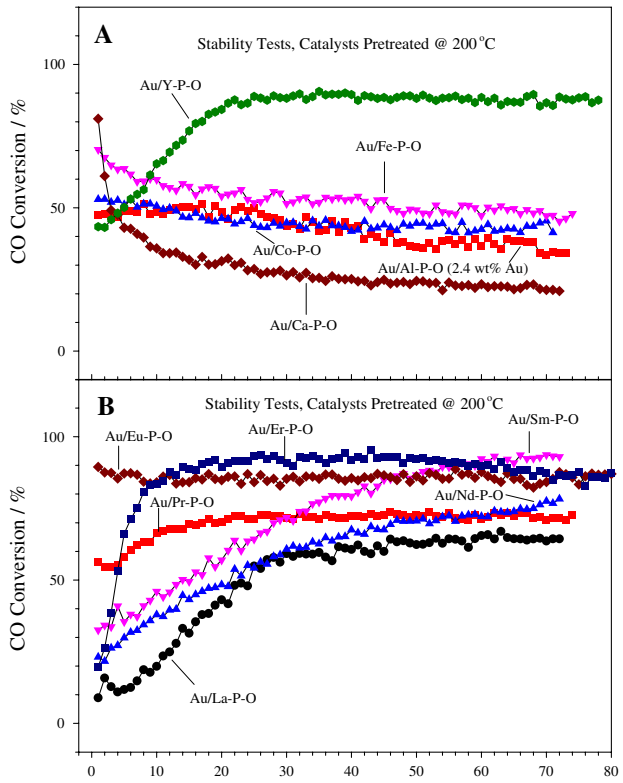

Fig. 9 Room-temperature CO conversions of 200 °C-pretreated Au/M–P–O catalysts as a function of time on stream

temporal activation of certain catalysts may be due to the accumulation of adsorbed water that may increase the CO conversion [52]. Note that the water vapor level of the as-supplied 1% CO is less than 4 ppm, so it takes hours to reach adsorption-desorption equilibrium at room temperature. To further verify our hypothesis, we pretreated Au/Sm–P–O in O_2-He at 500 °C, cooled it down to room temperature, let the O_2-He flow through the catalyst for 3 days, and then measured the CO conversion as a function of time on stream. As shown in Fig. S7, the initial induction period is significantly shortened (Fig. S7).

4 Discussion and Conclusions

In a previous communication [26], our group communicated that gold nanoparticles supported on nanosized $LaPO_4$ (6–8 nm) are active for CO oxidation. However, it was not clear from that communication whether the use of $LaPO_4$ as the support is a serendipitous choice, or represents a general direction for further catalyst development. In fact, our group later found that gold nanoparticles on zeolite $AlPO_4$-H1 are not particularly active for CO oxidation [34]. The key contribution of our current work is not only to confirm the usefulness of $LaPO_4$ [26] in this regard, but also to demonstrate for the first time that a number of other metal phosphates can also be good supports for gold nanoparticles. It should be reiterated that the majority of the metal phosphate-supported gold catalysts developed herein have not been reported in the literature [1–5], and metal salt-based gold catalysts are scarce [22–27, 34].

Among the catalysts reported here, Au/M–P–O (M = Ca, Y, La, Pr, Nd, Sm, Eu, Ho, Er) catalysts show high CO conversions below 50 or 100 °C when they are pretreated in O_2-He at 200 or 500 °C. In particular, the specific rates of

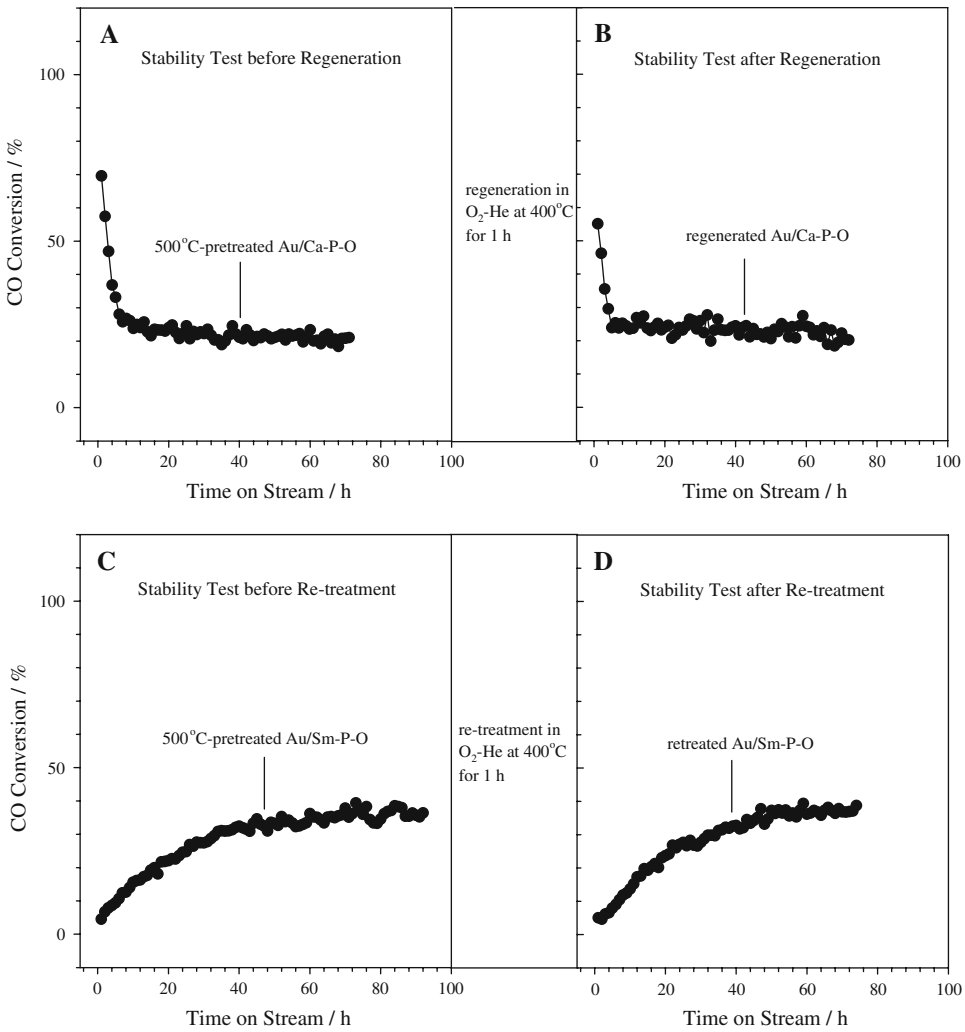

Fig. 10 Effect of regeneration and retreatment in O_2-He at 400 °C on the catalytic activity of 500 °C-pretreated Au/Ca–P–O and Au/Sm–P–O

200 °C-pretreated Au/M–P–O (M = La, Pr, and Ho) at 30 °C are calculated to be as high as 1.9, 1.9, and 2.3 mmol g_{Au}^{-1} h^{-1}, respectively. Au/M–P–O (M = Mg, Al, Zn, Zr) catalysts are always not particularly active, regardless of the pretreatment temperature. On the other hand, Au/M–P–O (M = Fe, Co) catalysts are active after 200 °C-pretreatment, but significantly deactivate after 500 °C-pretreatment. Although 200 °C-pretreated Au/M–P–O catalysts show lower CO conversions than 200 °C-pretreated Au/TiO_2, many active Au/M–P–O catalysts can withstand high-temperature treatment without dramatic loss of activity. Sizes of gold nanoparticles may play an important role in determining catalytic activity, but support effect is also important.

It should be mentioned that the scope of the current work is to screen new gold catalysts and develop new catalyst systems, whereas the other technical details (e.g., influences of gold loadings, pH values, delicately synthesized supports) may be systematically studied in the future. We believe that the development of such new catalyst system (metal phosphate-based gold catalysts) is important because further research can be carried out to elucidate the nature of active sites and to use these catalysts to run new reactions. Although herein we used CO oxidation as a probe reaction to screen the activity of new gold catalysts, we believe that our new catalysts should be useful in organic catalysis, considering that gold nanoparticles may catalyze oxidation and hydrogenation reactions [1–5] whereas metal phosphates possess acid-base and oxidation properties [20, 28–32].

Acknowledgements This work was supported by the Office of Basic Energy Sciences, U.S. Department of Energy. The Oak Ridge National Laboratory is managed by UT-Battelle, LLC for the U.S. DOE under Contract DE-AC05-00OR22725. This research was supported in part by the appointment for Z. Ma and H.F. Yin to the ORNL Research Associates Program, administered jointly by ORNL and the Oak Ridge Associated Universities.

References

1. Haruta M, Daté M (2001) Appl Catal A 222:427
2. Choudhary TV, Goodman DW (2002) Top Catal 21:25

3. Hashmi ASK, Hutchings GJ (2006) Angew Chem Int Ed 45:7896
4. Bond GC, Louis C, Thompson DT (2006) Catalysis by gold. Imperial College, London
5. Kung MC, Davis RJ, Kung HH (2007) J Phys Chem C 111:11767
6. Schubert MM, Hackenberg S, van Veen AC, Muhler M, Plzak V, Behm RJ (2001) J Catal 197:113
7. Overbury SH, Ortiz-Soto L, Zhu HG, Lee B, Amiridis MD, Dai S (2004) Catal Lett 95:99
8. Delannoy L, El Hassan N, Musi A, Le To NN, Krafft J-M, Louis C (2006) J Phys Chem B 110:22471
9. Han Y-F, Zhong ZY, Ramesh K, Chen F, Chen L (2007) J Phys Chem C 111:3163
10. Yan WF, Ma Z, Mahurin SM, Jiao J, Hagaman EW, Overbury SH, Dai S (2008) Catal Lett 121:209
11. Wen L, Fu J-K, Gu P-Y, Yao B-X, Lin Z-H, Zhou J-Z (2008) Appl Catal B 79:402
12. Okumura M, Nakamura S, Tsubota S, Nakamura T, Azuma M, Haruta M (1998) Catal Lett 51:53
13. Okumura M, Tsubota S, Haruta M (2003) J Mol Catal A 199:73
14. Yang C-M, Kalwei M, Schüth F, Chao K-J (2003) Appl Catal A 254:289
15. Chi Y-S, Lin H-P, Mou C-Y (2005) Appl Catal A 284:199
16. Budroni G, Corma A (2006) Angew Chem Int Ed 45:3328
17. Zhu HG, Liang CD, Yan WF, Overbury SH, Dai S (2006) J Phys Chem B 110:10842
18. Zhu HG, Ma Z, Clark JC, Pan ZW, Overbury SH, Dai S (2007) Appl Catal A 326:89
19. Yin HF, Ma Z, Overbury SH, Dai S (2008) J Phys Chem C 112:8349
20. Tanabe K, Misono M, Ono Y, Hattori H (1989) New acids and bases. Elsevier, Amsterdam
21. Deng XY, Ma Z, Yue YH, Gao Z (2001) J Catal 204:200
22. Lian HL, Jia MJ, Pan WC, Li Y, Zhang WX, Jiang DZ (2005) Catal Commun 6:47
23. Venugopal A, Scurrell MS (2003) Appl Catal A 245:137
24. Phonthammachai N, Zhong ZY, Guo J, Han YF, White TJ (2008) Gold Bull 41:42
25. Han Y-F, Phonthammachai N, Ramesh K, Zhong ZY, White T (2008) Ind Eng Chem Res 42:908
26. Yan WF, Brown S, Pan ZW, Mahurin SM, Overbury SH, Dai S (2006) Angew Chem Int Ed 45:3614
27. Liu JF, Chen W, Liu XW, Zhou KB, Li YD (2008) Nano Res 1:46
28. Takita Y, Sano K, Kurosaki K, Kawata N, Nishiguchi H, Ito M, Ishihara T (1998) Appl Catal A 167:49
29. Takita Y, Sano K, Muraya T, Nishiguchi H, Kawata N, Ito M, Akbay T, Ishihara T (1998) Appl Catal A 170:23
30. Ai M (2003) Catal Today 85:193
31. Bautista FM, Campelo JM, García A, Luna D, Marinas JM, Quirós RA, Romero AA (2003) Appl Catal A 243:93
32. Bautista FM, Campelo JM, Luna D, Marinas JM, Quirós RA, Romero AA (2007) Appl Catal B 70:611
33. Kosmulski M (ed) (2001) Chemical properties of material surfaces. Marcel Dekker, New York
34. Yan WF, Chen B, Mahurin SM, Overbury SH, Dai S (2007) Stud Surf Sci Catal 170:1065
35. Li MJ, Wu ZL, Ma Z, Schwartz V, Mullins DR, Dai S, Overbury SH (2008) in preparation
36. Corti CW, Holliday RJ, Thompson DT (2005) Appl Catal A 291:253
37. Corti CW, Holliday RJ, Thompson DT (2007) Top Catal 44:331
38. Min BK, Wallace WT, Santra AK, Goodman DW (2004) J Phys Chem B 108:16339
39. Kielbassa S, Kinne M, Behm RJ (2004) J Phys Chem B 108:19184
40. Ma Z, Brown S, Overbury SH, Dai S (2007) Appl Catal A 327:226
41. Ma Z, Overbury SH, Dai S (2007) J Mol Catal A 273:186
42. Zhu HG, Ma Z, Overbury SH, Dai S (2007) Catal Lett 116:128
43. Ma Z, Brown S, Howe JY, Overbury SH, Dai S (2008) J Phys Chem C 112:9448
44. Nagaraju P, Srilakshmi C, Pasha N, Lingaiah N, Suryanarayana I, Sai Prasad PS (2008) Appl Catal A 334:10
45. Bond GC, Thompson DT (2000) Gold Bull 33:41
46. Knell A, Barnickel P, Baiker A, Wokaun A (1992) J Catal 137:306
47. Haruta M (2002) Cattech 6:102
48. Schumacher B, Plzak V, Kinne M, Behm RJ (2003) Catal Lett 89:109
49. Konova P, Naydenov A, Venkov C, Mehandjiev D, Andreeva D, Tabakova T (2004) J Mol Catal A 213:235
50. Konova P, Naydenov A, Tabakova T, Mehandjiev D (2004) Catal Commun 5:537
51. Wu ZL, Zhou SH, Zhu HG, Dai S, Overbury SH (2008) Chem Commun 3308
52. Daté M, Okumura M, Tsubota S, Haruta M (2004) Angew Chem Int Ed 43:2129